

## Strain-Engineered Multiferroicity in $Pnma$ $\text{NaMnF}_3$ Fluoroperovskite

A. C. Garcia-Castro,<sup>1,2,\*</sup> A. H. Romero,<sup>3,2,†</sup> and E. Bousquet<sup>1,‡</sup>

<sup>1</sup>*Physique Théorique des Matériaux, Université de Liège, B-4000 Sart-Tilman, Belgium*

<sup>2</sup>*Centro de Investigación y Estudios Avanzados del IPN, MX-76230 Querétaro, Mexico*

<sup>3</sup>*Physics Department, West Virginia University, Morgantown, West Virginia 26506-6315, USA*

(Received 9 September 2015; published 14 March 2016)

In this study we show from first principles calculations the possibility to induce multiferroic and magnetoelectric functional properties in the  $Pnma$   $\text{NaMnF}_3$  fluoroperovskite by means of epitaxial strain engineering. Surprisingly, we found a very strong nonlinear polarization-strain coupling that drives an atypical amplification of the ferroelectric polarization for either compression or expansion of the cell. This property is associated with a noncollinear antiferromagnetic ordering, which induces a weak ferromagnetism phase and makes the strained  $\text{NaMnF}_3$  fluoroperovskite multiferroic. The magnetoelectric response was calculated and it was found to be composed of linear and nonlinear components with amplitudes similar to the ones of  $\text{Cr}_2\text{O}_3$ . These findings show that it is possible to move the fluoride family toward functional applications with unique responses.

DOI: 10.1103/PhysRevLett.116.117202

search for new and innovative materials with promising multifunctional multiferroic (MF) properties has been one of the keystones of condensed matter research in the last decade [1,2]. Several systems and compounds based on oxide perovskites have been reported as ideal candidates. In these systems, even in the absence of a ferroic order at the bulk level, physical constrains such as biaxial epitaxial strain in thin films can be used to artificially induce a ferroelectric (FE) order [3]. This has been successfully performed in paraelectric crystals such as  $\text{SrTiO}_3$  [4] or  $\text{CaTiO}_3$  [5]. A similar mechanism has been reported for magnetic perovskites [6–8], and thus exceeding the so-called  $d^0$ -ness rule that is expected to prevent the formation of a FE phase in magnetic perovskites [9]. However, the possibility for new materials with MF properties in new stoichiometries away from the easily polarizable oxides is still evasive. Scott and Blinc have reported several other possible and unexplored MF and magnetoelectric (ME) candidates in the fluoride crystal class of materials [10]. Nonetheless, none of the reported fluoride candidates belong to the most claimed perovskite family. Recently, we have shown that even if none of the fluoroperovskites are reported with a FE ground state (except  $\text{CsPbF}_3$  [11,12]) they have nevertheless the propensity to have a FE instability in their high symmetry cubic reference structure [13]. We have identified that the FE instability of the fluoroperovskites is related to a steric geometric effect when small cations lie at the  $A$  site. The latter is at the origin of the mechanism reported in rare-earth compounds (e.g.,  $\text{RGaO}_3$ ,  $\text{RInO}_3$  [14]), double perovskites (e.g.,  $\text{La}_2\text{NiMnO}_6$  [15]), and “ferroelectric metals” (e.g.,  $\text{LiOsO}_3$  [16,17]) involving an  $A$ -site dominated effect, but it is different from the  $A$ -site stereochemically active lone pair origin observed in some oxides (e.g.,  $\text{PbTiO}_3$  or

$\text{BiFeO}_3$ ) oxides and from the phonon mode coupling origin present in improper and hybrid-improper FE [18]. Unfortunately, these fluoroperovskites keep the “undesired” competition between the FE and antiferrodistortive (AFD) instabilities, AFD instabilities dominate in the bulk ground states. Interestingly, and similarly to the oxides, we have shown that by applying epitaxial strain, FE orders in fluoroperovskites can be induced. Therefore, this observation opens a new path to discover novel ferroelectrics of geometric origin in ionic crystals. In this Letter, we explore from first-principles the properties of strain-induced ferroelectricity and multiferroism in  $\text{NaMnF}_3$  and find breakthrough differences with the oxides. Interestingly, we show that the geometric origin of the ferroelectricity drives unique responses such as a nonlinear strain-polarization coupling that is associated with a very strong second order piezoelectric response and a nonlinear ME effect. We also predict a very strong spin canting in the antiferromagnetic  $\text{NaMnF}_3$  crystal that drives a sizable ferromagnetic component and thus making strained  $\text{NaMnF}_3$  a good MF candidate. All of that shows that engineering ferroelectricity and multiferroism in the fluoroperovskite class of materials is very appealing to discover unexplored multifunctional properties with unprecedented responses.

We used density functional theory (DFT) within the projected augmented-waves (PAW) [19] method as implemented in VASP [20,21]. The exchange correlation was represented within the generalized gradient approximation (GGA) by the PBEsol parameterization [22] and corrected with the DFT +  $U$  method [23] ( $U = 4.0$  eV) in order to treat the localized  $d$  electrons of Mn. The periodic solution of these crystalline structures was represented by using Bloch states with a Monkhorst-Pack  $k$ -point mesh of  $6 \times 4 \times 6$  and 700 eV energy cutoff, which give forces

converged to less than 1 meV  $\text{\AA}^{-1}$ . The spin-orbit coupling (SOC) was included to simulate the noncollinear calculations [24]. Born effective charges and phonon calculations were performed with density-functional perturbation theory (DFPT) [25] as implemented in VASP. The FE spontaneous polarization was computed through the Berry phase approach [26]. The ME coupling was obtained by computing the spontaneous polarization as a function of the applied Zeeman magnetic field as implemented by Bousquet *et al.* [27] within the local density approximation (LDA) approach [28]. We have evaluated the ME response against the  $U$  and  $J$  parameters of the DFT +  $U$  method (see Supplemental Material [29]) and found that besides amplitude modifications, the global qualitative picture stays the same and it is thus much less dramatic than what has been reported in Ref. [30].

NaMnF<sub>3</sub> crystallizes in the  $Pnma$  (group No. 62) structure at room conditions. Within our DFT calculations we obtained relaxed cell parameters  $a_0 = 5.750$   $\text{\AA}$ ,  $b_0 = 8.007$   $\text{\AA}$ , and  $c_0 = 5.547$   $\text{\AA}$  in good agreement with experimental reports by Daniel *et al.* [31] with a maximum error of 0.2%. This nonpolar ground state is coming from the condensation of AFD modes and antipolar displacements of the Na atoms such as the FE instability observed in the cubic phase [13] is suppressed by the AFD ones. Thus, the competition between FE, antipolar displacements and AFD distortions monitors the  $Pnma$  phase but the balance between them is delicate in the case of NaMnF<sub>3</sub> since we still find a very soft  $B_{2u}$  polar mode at 18  $\text{cm}^{-1}$ . This means that the  $Pnma$  phase is very close to being FE and thus close to being an incipient ferroelectric [32]. This property can be verified experimentally.

*Ferroelectric behavior in strained NaMnF<sub>3</sub>.*—In FE oxides it is well known that the epitaxial strain can induce ferroelectricity in the  $Pnma$  phase [5,8] or enhance it in FE compounds such as PbTiO<sub>3</sub> or BiFeO<sub>3</sub> [3,6]. Here we show that a similar strain-engineered ferroelectricity can be used in NaMnF<sub>3</sub>. We suppose a cubic perovskite substrate ( $a_c$ ) as the source of the strain by imposing the  $Pnma$  symmetry into the crystal  $a = c = \sqrt{2}a_c$ . We choose the 0% strain reference to be  $a_r = (a_0 + c_0)/2$  with  $a_0$  and  $c_0$  the unstrained relaxed cell parameters of the  $Pnma$  phase and defining the strain amplitude by  $\varepsilon = (a - a_r)/a_r$ . In this configuration the soft  $B_{2u}$  mode is polarized perpendicular to the biaxial strain (i.e., along the orthorhombic  $b$  axis).

In Fig. 1(a) we plot the evolution of the  $B_{2u}$  mode frequency with respect to the epitaxial strain. Unexpectedly, we see that the  $B_{2u}$  mode becomes unstable *whatever* the value of the epitaxial strain is, in compression or in expansion. This means that for any value of the epitaxial strain, NaMnF<sub>3</sub> has a FE instability. After condensing this modes by taking different amplitudes of it, we obtain a double well barrier energy plotted in Fig. 1(c), which shows that for either positive or negative strain

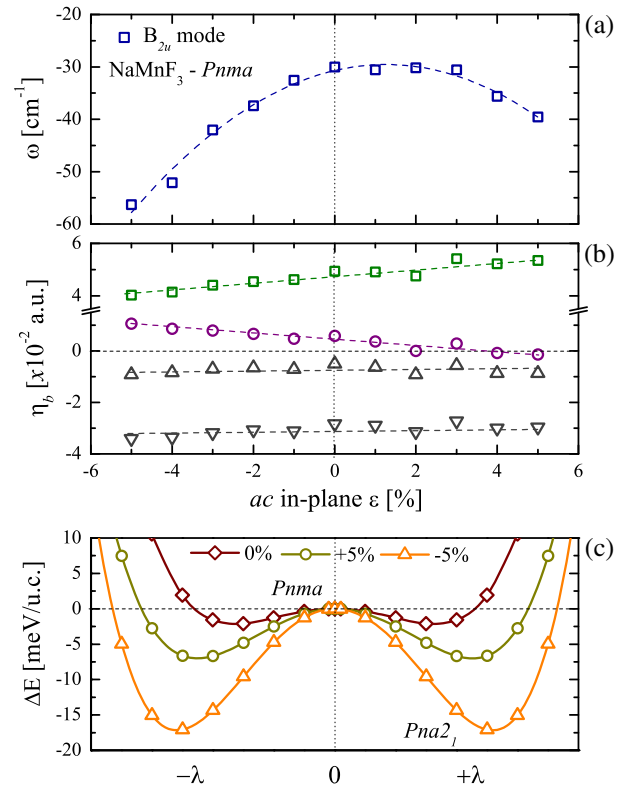


FIG. 1. (a) Frequency of the polar  $B_{2u}$  unstable mode of  $Pnma$  NaMnF<sub>3</sub> with respect to the epitaxial strain (imaginary frequencies are represented as negative values). (b)  $B_{2u}$  mode eigendisplacement contributions of each atomic type (Na in green squares, Mn in purple circles, and  $F_{\perp}$ ,  $F_{\parallel}$  in up and down gray triangles, respectively). (c) Energy versus freezing-in amplitude of the  $B_{2u}$  mode for 0%, +5%, and -5% strain values, which shows that expansion or compression enlarges ferroelectricity.

amplitudes, the FE double well is amplified. When performing the structural relaxations, we indeed find a FE ground state with the  $Pna2_1$  space group (No. 33) for all strain values. Then, the ground state of epitaxially constrained NaMnF<sub>3</sub> is always FE and thus MF due to the magnetically active  $\text{Mn}^{+2}$  cation. The strain-induced ferroelectricity in  $Pnma$  perovskites is well established in oxides [4,5,8] and can thus be extended to the fluoride family but with the following striking differences. The first one is that the polarization is enhanced for positive or negative values of the strain while in oxides the relationship is linear, in such a way that if one direction of strain enhances the FE polarization, it reduces and destroys it on the opposite direction [3]. A second difference is that the polarization develops in the direction where the antipolar motions of the Na atoms ( $X_5^+$  mode) are absent. This property is related to the geometric origin of the polar instability in fluoroperovskites. The Na is strongly unstable due to the loss of bonding of this small cation in a large unit cell. This loss of bonding is relaxed by the motion of the Na away from its high symmetry position through polar or antipolar motions. In the  $Pnma$  phase this is done through

antipolar motions along the  $a$  and  $c$  directions, but along the  $b$  direction the loss of bonding is still present and it is the source of the softness of the polar  $B_{2u}$  mode along the  $b$  direction.

To understand the origin of these unusual FE responses, we analyzed the eigendisplacement ( $\eta_b$ ) changes of the unstable mode  $B_{2u}$  under epitaxial strain [see Fig. 1(b)]. We can see that the Na contribution is reduced when going from positive to negative values of the strain while it is the opposite for the Mn atom, the fluorine contributions being unchanged in the same range. This means that the change of mode frequency is related to the change in the eigendisplacement pattern from Na dominated to Na + Mn dominated.

In Fig. 2 we report the evolution of the polarization versus the epitaxial strain. Here again, we observe an unusual and outstanding polarization-strain coupling in which the nonlinear contribution dominates the linear one. This can be expressed in terms of the strain, piezoelectric constants, and polarization as follows:

$$P_\mu = \sum_j e_{\mu j} \varepsilon_j + \frac{1}{2} \sum_{j,k} B_{\mu jk} \varepsilon_j \varepsilon_k, \quad (1)$$

where  $P_\mu$  is the spontaneous polarization (with  $\mu = 1, 2, 3$  for the cartesian components  $x, y, z$  respectively),  $\varepsilon_j$  ( $j = 1, 2, \dots, 6$  as the components of the tensor in Voigt notation) is the strain tensor, and  $e_{\mu j}$ ,  $B_{\mu jk}$  are the linear and quadratic piezoelectric coefficients, respectively. The computed linear piezoelectric coefficients  $e_{21}$ ,  $e_{23}$ ,  $e_{22}$ ,  $e_{16}$ , and  $e_{34}$  at 0% strain are equal to 1.010,  $-0.672$ ,  $0.064$ ,  $-0.108$ , and  $0.058$  C m $^{-2}$ , respectively, and are not far from the ones observed in BaTiO $_3$  [33,34]. From the quadratic fitting observed in Fig 2, we can extract that the overall nonlinear contribution related to the sum of the  $B_{\mu jk}$  components and we found it to be about 60% of the linear

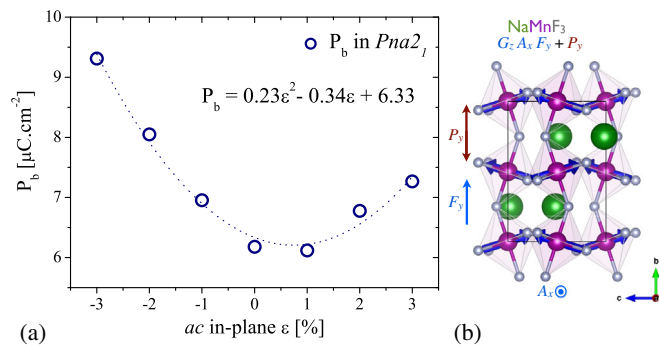


FIG. 2. (a) Evolution of the polarization along  $b$  axis of  $Pna2_1$  NaMnF $_3$  with respect to the epitaxial strain. An unusual nonlinear polarization strain coupling is observed and can be associated with a nonlinear piezoelectric response. (b) Schematic view of the  $Pna2_1$  NaMnF $_3$  structure in which Na, Mn, and F ions are depicted in green, violet, and grey, respectively. The noncollinear magnetic ground state (large arrows going through the Mn), the direction of the cantings as well as the electric polarization along the  $b$  axis are also pictured.

piezoelectric constants ( $e_{\mu j}$ ). This large nonlinear piezoelectric response is very unique to the steric geometric origin of the ferroelectricity. In order to check this hypothesis, we have plotted the polarization vs strain for another steric geometric FE compound (BaCoF $_4$ ), and for regular FE (BaTiO $_3$ ) and improper FE (PbTiO $_3$ /SrTiO $_3$  superlattice) systems (see Supplemental Material [29]). Interestingly, the strong nonlinear polarization-strain coupling is only observed for the steric geometric FE crystals, which confirms that this property is unique to geometric FE systems and promises thus to enlarge the small family of nonlinear piezoelectrics such as the zinc-blende semiconductors [35].

*Noncollinear magnetism and ME coupling in Pna2 $_1$  NaMnF $_3$ .*—In the following section, we analyze the magnetic properties of strained NaMnF $_3$ . The possible allowed magnetic orderings and couplings were obtained based on group theory analysis [36], which we report in Table I. We note that in the  $Pna2_1$  phase, whatever the magnetic state adopted by the system is, spin canting and ME responses are allowed by symmetry. A predominant  $G$ -type antiferromagnetism (AFM) behavior with spin canting driving a weak magnetization along  $b$  axis [37] has been experimentally observed in the  $Pnma$  phase. Our noncollinear calculations give the same noncollinear magnetic ground state with a marked  $G$ -type AFM along the  $c$  axis,  $A$ -type AFM canting along the  $a$  direction, and a ferromagnetic canting along the  $b$  direction ( $A_x F_y G_z$  in Bertaut's notation). In the strained  $Pna2_1$  phase we do not observe a magnetic transition, implying that the system always remains in the  $G_z A_x F_y$  noncollinear ground state. The ferromagnetic canting gives a magnetization of  $0.02 \mu_B$ /atom, which is 1 order of magnitude larger than the one found in CaMnO $_3$  ( $0.004 \mu_B$ /atom [8]).

The related magnetic point group ( $m' m' 2$ ) of the  $A_x F_y G_z$  magnetic ground state, allows for linear and nonlinear ME response [40] while the energy expansion can be written as

$$P_i = \alpha_{ik} H_k + \frac{1}{2} \beta_{ijk} H_j H_k + \gamma_{jik} H_j E_k, \quad (2)$$

where  $P_i$  is the spontaneous ferroelectric polarization along each particular Cartesian axis ( $i = x, y, \text{ and } z$ ),  $H_k$  is the applied magnetic field along the  $k$  axis, and  $\alpha_{ik}$  and  $\beta_{ijk}/\gamma_{jik}$  are the linear and nonlinear ME tensor components, respectively.

TABLE I. Allowed magnetic orderings and ME response in the  $D_{2h}$  point symmetry group [38,39] of the  $Pna2_1$  phase.

Magnetic Ordering	Character	$Pna2_1$	
		Linear ME	Second order ME
$C_x, G_y, F_z$	$A_2$	$\alpha_{yz}, \alpha_{zy}$	$\beta_{ijk}, \gamma_{jik}$
$A_x, F_y, G_z$	$B_1$	$\alpha_{xx}, \alpha_{yy}, \alpha_{zz}$	$\beta_{ijk}, \gamma_{jik}$
$F_x, A_y, C_z$	$B_2$	$\alpha_{xz}, \alpha_{zx}$	$\beta_{ijk}, \gamma_{jik}$
$G_x, C_y, A_z$	$A_1$	$\alpha_{xy}, \alpha_{yx}$	$\beta_{ijk}, \gamma_{jik}$

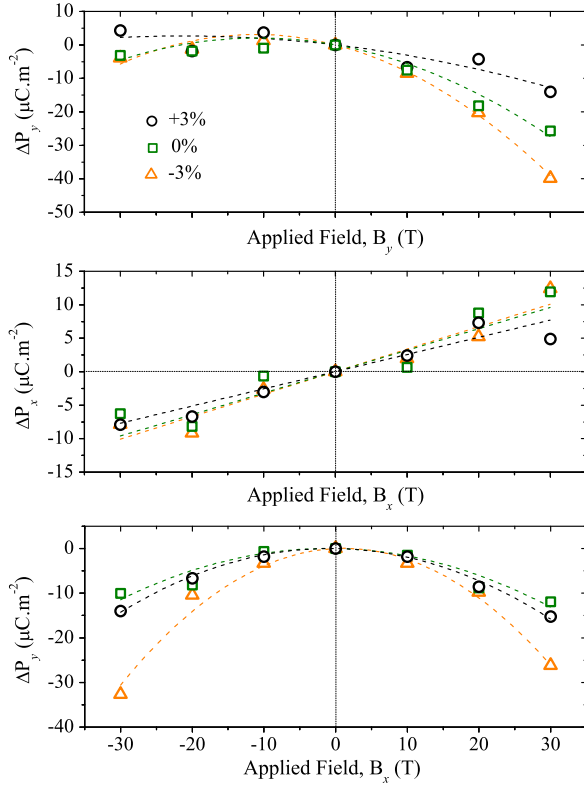


FIG. 3. Change of polarization ( $\Delta P_i$ ) versus magnetic field in strained  $\text{NaMnF}_3$  ( $Pna2_1$  phase). The dashed lines represent fitting curves following Eq. (2). The second-order ME coupling can be appreciated from the figure, for fields applied along  $x$  and  $y$  directions an increase of the nonlinear behavior is observed when strain goes from positive to negative values. The first and second order ME tensor components computed from these plots are presented in the Table II.

In Fig. 3 we report the evolution of the electric polarization with respect to the amplitude of the applied magnetic field along different directions. In Table II we report the extracted ME coefficients at three different epitaxial strains. Our results reveal that a sizable nonlinear ME coupling is present when the magnetic field is applied along the  $y$  axis (parallel to the weak-FM moment). When the field is applied along the  $x$  axis, we observe a linear ME response along the same direction ( $\alpha_{xx}$ ) and a nonlinear one along the  $y$  axis ( $\beta_{yxx}$ ). The amplitude of the linear ME response of strained  $\text{NaMnF}_3$  is close to the one reported in  $\text{Cr}_2\text{O}_3$  [41–44]. All the ME coefficients increase when the strain goes from positive to negative values, which is

TABLE II. ME coefficients of strained  $\text{NaMnF}_3$  expressed as in Eq. (2),  $\alpha_{ik}$  in [ $\text{ps m}^{-1}$ ] and  $\beta_{jik}$  in [ $\times 10^{-8} \text{ ps A}^{-1}$ ].

$\epsilon$ [%]	$\alpha_{yy}$	$\alpha_{xx}$	$\beta_{yyy}$	$\beta_{xxx}$	$\beta_{yxx}$
+3%	-0.314	0.322	-0.927	0.000	-2.625
0%	-0.480	0.403	-2.232	0.000	-2.156
-3%	-0.698	0.423	-3.931	0.000	-4.973

consistent with the fact that the polarization contribution of the magnetic Mn atoms is larger for compressive strains and thus we can expect a stronger coupling between electric polarization and magnetism. Additionally, the global forms of the ME responses in this fluoroperovskite are very similar to the ones predicted for  $\text{CaMnO}_3$  [8], which shows that this might be a general rule for strain-induced ferroelectricity in the  $Pnma$  structure. We note that the ME response is observed in spite of a non-Mn-driven polar distortion. When projecting the  $B$ -field induced distortions against the  $Pnma$  phonon modes' basis set (see Supplemental Material [29]) we found that at compressive strains the unstable polar  $B_{2u}$  mode is the one contributing the most to the ME distortions, in agreement with the fact that at compressive strain the character of the polar unstable mode becomes Mn driven [see Fig. 1(b)] and with the fact that the ME response is larger for compressive strain (as shown in Table II). We also note that several higher frequency  $A_g$  and  $B_{2u}$  modes also strongly contribute to the  $B$ -field induced distortions, which means that the ME response is also related to phonon mode distortions that are different than the one responsible for the spontaneous ferroelectric polarization, this mechanism being dominant for tensile strains [27].

From the industrial point of view, fluorides have proved to be of high interest for numerous long term applications, such as fluoride-based glasses with a large thermal expansion, a low refractive and nonlinear index [45,46], strong magnets with an optical transparency in the visible light [47,48], electrochemical devices, solid-state batteries, gas sensors, and electrochromic systems [49] or catalyst surfaces in the base of metal fluorides such as  $\text{AlF}_3$  [50]. Thus, adding multiferroic properties in fluoroperovskites would open an exciting opportunity to their use in novel and extended applications.

In this Letter we have shown from first principles calculations that a multiferroic ground state can be induced in  $\text{NaMnF}_3$  thin films through epitaxial strain with an unprecedented nonlinear polarization-strain coupling. This unusual polarization-strain coupling is related to the specific geometric source of ferroelectricity of this ionic crystal and further analysis should be performed on other similar systems in order to confirm the rule (for example in the  $\text{BaMF}_4$  family). We have shown that this unique multiferroic state drives a large and uncommon second order piezoelectric response and a nonlinear magnetoelectric response. We hope our results will motivate further theoretical and experimental studies owing to the fact that making a fluoroperovskite multiferroic is a primer and it would open the field of multifunctional materials to new candidates with novel and remarkable responses.

This work used the Extreme Science and Engineering Discovery Environment (XSEDE), which is supported by National Science Foundation Grant No. OCI-1053575. In Belgium, the computational resources have been provided by the Consortium des Equipements de Calcul Intensif

(CECI), funded by the F.R.S.-FNRS under Grant No. 2.5020.11. Additionally, the authors acknowledge the support from the Texas Advances Computer Center (TACC) with the Stampede supercomputer. This work was supported by FRS-FNRS Belgium (E. B.), DMREF-NSF 1434897 (A. R.) and the Donors of the American Chemical Society Petroleum Research Fund for partial support of this research under Contract No. 54075-ND10 (A. R.).

\*a.c.garcia.castro@gmail.com

†alromero@mail.wvu.edu

‡eric.bousquet@ulg.ac.be

- [1] W. Eerenstein, N. D. Mathur, and J. F. Scott, *Nature (London)* **442**, 759 (2006).
- [2] L. Martin, Y.-H. Chu, and R. Ramesh, *Mater. Sci. Eng. R* **68**, 89 (2010).
- [3] O. Diéguez, K. M. Rabe, and D. Vanderbilt, *Phys. Rev. B* **72**, 144101 (2005).
- [4] J. Haeni *et al.*, *Nature (London)* **430**, 758 (2004).
- [5] C.-J. Eklund, C. J. Fennie, and K. M. Rabe, *Phys. Rev. B* **79**, 220101 (2009).
- [6] C. Ederer and N. A. Spaldin, *Phys. Rev. Lett.* **95**, 257601 (2005).
- [7] T. Günter, E. Bousquet, A. David, P. Boullay, P. Ghosez, W. Prellier, and M. Fiebig, *Phys. Rev. B* **85**, 214120 (2012).
- [8] E. Bousquet and N. Spaldin, *Phys. Rev. Lett.* **107**, 197603 (2011).
- [9] N. A. Hill, *J. Phys. Chem. B* **104**, 6694 (2000).
- [10] J. F. Scott and R. Blinc, *J. Phys. Condens. Matter* **23**, 113202 (2011).
- [11] P. Berastegui, S. Hull, and S.-G. Eriksson, *J. Phys. Condens. Matter* **13**, 5077 (2001).
- [12] E. H. Smith, N. A. Benedek, and C. J. Fennie, *Inorg. Chem.* **54**, 8536 (2015).
- [13] A. C. Garcia-Castro, N. A. Spaldin, A. H. Romero, and E. Bousquet, *Phys. Rev. B* **89**, 104107 (2014).
- [14] T. Tohei, H. Moriwake, H. Murata, A. Kuwabara, R. Hashimoto, T. Yamamoto, and I. Tanaka, *Phys. Rev. B* **79**, 144125 (2009).
- [15] R. Takahashi, I. Ohkubo, K. Yamauchi, M. Kitamura, Y. Sakurai, M. Oshima, T. Oguchi, Y. Cho, and M. Lippmaa, *Phys. Rev. B* **91**, 134107 (2015).
- [16] H. M. Liu, Y. P. Du, Y. L. Xie, J.-M. Liu, C.-G. Duan, and X. Wan, *Phys. Rev. B* **91**, 064104 (2015).
- [17] N. A. Benedek and T. Birol, *J. Mater. Chem. C* (2016).
- [18] J. Young, A. Stroppa, S. Picozzi, and J. M. Rondinelli, *J. Phys. Condens. Matter* **27**, 283202 (2015).
- [19] P. E. Blöchl, *Phys. Rev. B* **50**, 17953 (1994).
- [20] G. Kresse and J. Furthmüller, *Phys. Rev. B* **54**, 11169 (1996).
- [21] G. Kresse and D. Joubert, *Phys. Rev. B* **59**, 1758 (1999).
- [22] J. P. Perdew, A. Ruzsinszky, G. I. Csonka, O. A. Vydrov, G. E. Scuseria, L. A. Constantin, X. Zhou, and K. Burke, *Phys. Rev. Lett.* **100**, 136406 (2008).
- [23] A. I. Liechtenstein, V. I. Anisimov, and J. Zaanen, *Phys. Rev. B* **52**, R5467 (1995).
- [24] D. Hobbs, G. Kresse, and J. Hafner, *Phys. Rev. B* **62**, 11556 (2000).
- [25] X. Gonze and C. Lee, *Phys. Rev. B* **55**, 10355 (1997).
- [26] D. Vanderbilt, *J. Phys. Chem. Solids* **61**, 147 (2000).
- [27] E. Bousquet, N. A. Spaldin, and K. T. Delaney, *Phys. Rev. Lett.* **106**, 107202 (2011).
- [28] The implementation under the GGA approach gives unphysical results in both VASP and ABINIT packages. Its correction is under way by the authors.
- [29] See Supplemental Material at <http://link.aps.org/supplemental/10.1103/PhysRevLett.116.117202> for dependence of the spontaneous polarization as a function of epitaxial strain for several ferroelectric systems. Activation of modes by an applied magnetic field and dependence of the ME-coupling under the DFT +  $U$  +  $J$  formalism.
- [30] E. Bousquet and N. Spaldin, *Phys. Rev. B* **82**, 220402 (2010).
- [31] P. Daniel, M. Rousseau, A. Desert, A. Ratuszna, and F. Ganot, *Phys. Rev. B* **51**, 12337 (1995).
- [32] K. M. Rabe, C. H. Ahn, and J.-M. Triscone, *Physics of Ferroelectrics* (Springer, New York, 2007), pp. 1–398.
- [33] S. Sanna, C. Thierfelder, S. Wippermann, T. P. Sinha, and W. G. Schmidt, *Phys. Rev. B* **83**, 054112 (2011).
- [34] T. Furuta and K. Miura, *Solid State Commun.* **150**, 2350 (2010).
- [35] G. Bester, X. Wu, D. Vanderbilt, and A. Zunger, *Phys. Rev. Lett.* **96**, 187602 (2006).
- [36] E. F. Bertaut, Spin Configurations of Ionic Structures: Theory and Practice, in *A Treatise on Modern Theory and Materials*, edited by G. T. Rado and H. Shul (Academic Press, New York, 1963), Vol. 3, p. 149.
- [37] J. R. Shane, *J. Appl. Phys.* **38**, 1280 (1967).
- [38] M. Aroyo, L. J. M. Perez-Mato, C. Capillas, E. Kroumova, S. Ivantchev, G. Madariaga, A. Kirov, and H. Wondratschek, *Zeitschrift für Kristallographie—Crystalline Materials* **221**, 15 (2009).
- [39] M. I. Aroyo, A. Kirov, C. Capillas, J. M. Perez-Mato, and H. Wondratschek, *Acta Cryst.* **A62**, 115 (2006).
- [40] A. S. Borovik-Romanov and H. Grimmer, Magnetic Properties, in *International Tables for Crystallography* (John Wiley & Sons, Ltd, Hoboken, 2006).
- [41] V. J. Folen, G. T. Rado, and E. W. Stalder, *Phys. Rev. Lett.* **6**, 607 (1961).
- [42] E. Kita, K. Siratori, and A. Tasaki, *J. Appl. Phys.* **50**, 7748 (1979).
- [43] H. Wiegelmann, A. G. M. Jansen, P. Wyder, J.-P. Rivera, and H. Schmid, *Ferroelectrics* **162**, 141 (1994).
- [44] J. Íñiguez, *Phys. Rev. Lett.* **101**, 117201 (2008).
- [45] J. J. Videau and J. Portier, in *Inorganic Solid Fluorides*, edited by P. Hagenmuller (Academic Press, New York, 1985), pp. 309–329.
- [46] J. Ravez, in *Inorganic Solid Fluorides*, edited by P. Hagenmuller (Academic Press, New York, 1985), pp. 469–475.
- [47] R. Wolfe, A. J. Kurtzig, and R. C. LeCraw, *J. Appl. Phys.* **41**, 1218 (1970).
- [48] J.-M. Dance and A. Tressaud, in *Inorganic Solid Fluorides*, edited by P. Hagenmuller (Academic Press, New York, 1985), pp. 371–394.
- [49] J.-M. Reau and J. Grannec, in *Inorganic Solid Fluorides*, edited by P. Hagenmuller (Academic Press, New York, 1985), pp. 423–467.
- [50] E. Kemnitz and S. Rudiger, High surface area metal fluorides as catalysts, in *Functionalized Inorganic Fluorides* (John Wiley and Sons, Ltd., New York, 2010), pp. 69–99.